Compact Telescoping Sample Manipulator for Ultra-High Vacuum

A senior design project submitted in partial fulfillment of the requirements for the degree of

Bachelor of Science

at

HARVARD UNIVERSITY

by

Robert A. Turner

S.B. Degree Candidate in Mechanical Engineering

Faculty Advisors: Jennifer Hoffman & Christian Matt

Harvard University School of Engineering and Applied Sciences

Cambridge, MA

April 5, 2019

Preface

Abstract

Scanning tunneling microscopes (STMs) are used to resolve the morphology and electronic structure of a material surface with atomic resolution. Key factors to achieve state of the art STM measurements are stability (i.e. decoupling from external noise sources), low temperatures (<10K) and ultra-high vacuum (UHV) conditions, which usually require a long sample transfer mechanism. However, such a long manipulator is a pendulum that acts as an antenna for acoustic and vibrational noise in the lab and couples the noise into the STM. Here we show the design, construction, and performance of a compact telescoping manipulator attached to an STM system. Our compact manipulator reduces noise coupling to the STM by shifting the resonant frequency away from commonly found acoustic and vibrational modes (typically 10s of Hz) and resonances of the vibration isolation systems (typically 1 - 3 Hz). In addition, our telescoping arm would be a useful tool for any UHV precision measurement system in a confined space.

Table of Contents

Table of Figures

1. Introduction and Background

Scanning tunneling microscopes (STMs) can resolve the real space morphology and electronic structure of a crystal surface at atomic length scales. In order to achieve such high precision measurements, the stability of the instrument is a key factor and the effect of external disturbances has to be minimized. Many STM experiments must be conducted under ultra-high vacuum (UHV) conditions and at cryogenic temperatures (< 10 K). Therefore, samples are transferred *in-situ* from room temperature environment into the cryostat which typically requires a transfer manipulator of 5 - 6 ft. in length due to the large thermal gradient. However, such a long manipulator is a pendulum that acts as an antenna for acoustic and vibrational noise in the lab which disturbs atomic resolution imaging.

This project designs and tests a telescoping manipulator in order to minimize the manipulator's impact on the noise level within the Hoffman Lab low temperature UHV STM. The long transfer manipulator which is currently installed on the system, shown in Figure 1, acts as an antenna to smallest external noise sources. Furthermore, its resonance frequencies are in a range which are important for scientific measurements and strongly disturb the isolation system, as explained in detail later. Due to its shorter dimension, a telescoping arm is less prone to external noise and also less prone to interacting with the isolation system. The design of the telescoping arm reduces the length to one third of the current manipulator's size. The advantages of such a design are that the arm is more rigid (sharper resonances) and that its resonance frequencies shift into a less important range, i.e. to higher frequencies.

Such a telescoping transfer manipulator has been developed by an STM group at the University of Maryland [1], but their design is limited to two telescoping sections. Inspired by this, this project explores and develops a new telescoping concept that allows for more telescoping sections which further improve vibration characteristics and shrink the manipulator length.

Many STM designs involve large transfer manipulators, and a telescopic arm would be advantageous for many research groups. With less vibrational noise on any given STM system, researchers would be able to measure with a higher resolution. Enhancing the resolution of the system would allow for observation of finer details of the sample surface topography and electronic structure. Reduced vibrational noise would also allow faster measurements with lower integration time. A telescoping arm would be a useful tool for any high precision measurement system operating in UHV due to its improved vibrational characteristics (e.g. STM, atomic force microscope (AFM), etc.).

Furthermore, a telescoping arm would be useful for any UHV system which is located in confined spaces due to its reduced dimensions (e.g. laboratories with low ceilings). Therefore, many research groups of different fields may be interested in such a product.

1.1. Background Research

Current techniques to reduce acoustic and vibration noise in an STM system include vibration isolation systems [2], active vibration cancelation [3], and the recently developed telescoping sample transfer arms [1].

Vibration isolation systems are the most commonly used solution to the problem of vibrational noise for STM and similar systems. Isolation systems can be found in the form of tables and rooms floating on air springs. The problem with any isolation system is that its effectiveness is frequency dependent and it is susceptible to noises of frequencies near its resonant frequency.

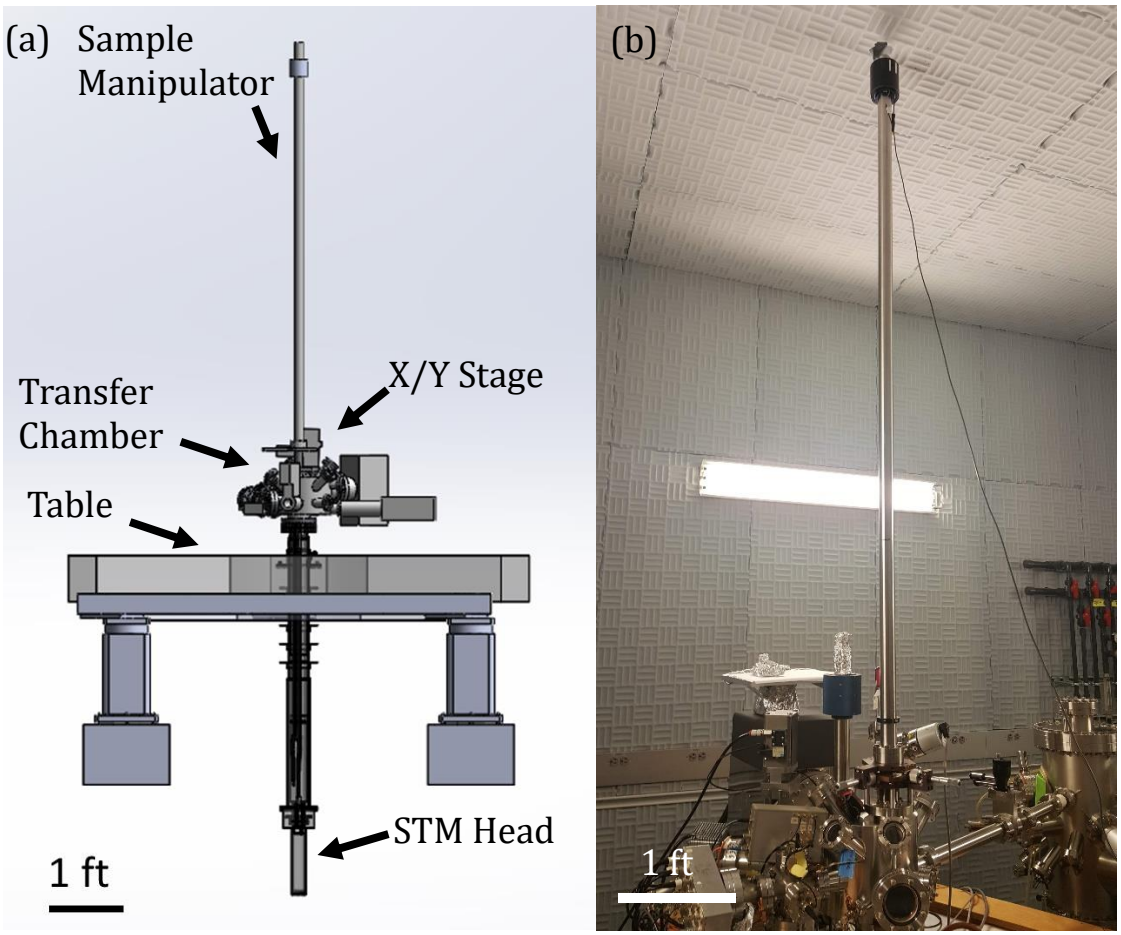

Figure 1: (a) CAD drawing of side view of the current Hoffman Lab low temperature UHV STM. A long, vertically mounted transfer manipulator is required to transfer samples into the STM head. **(b)** Photo of current transfer manipulator on an STM in the Hoffman Lab. Due to its long length it's prone to external noise.

Active vibration cancelation [3] is not commonly implemented into STM systems yet because of its high complexity and cost, but the technology is improving in its performance and compatibility with existing STMs.

The University of Maryland has taken an innovative approach and implemented a two-stage telescoping sample transfer arm [1]. Maryland's transfer arm reduces the arm's coupling to external noise sources and improves their vibrational spectrum by decreasing the height of their sample transfer arm. This is effective, but by only decreasing the height of the sample transfer arm by a factor of two, the success is limited. Maryland's joint locking mechanism also lacks the ability for automation of the sample transfer process.

Furthermore, Kurt J. Lesker Company has recently come out with their own commercialized linear telescopic transfer arm [4]. The commercialized arm is limited in that it lacks the ability for rotation and only has a maximum extension of ~ 1m in length.

A previous member of the Hoffman Lab inspired by the results of Maryland, came up with a conceptual design of a three to four stage telescoping sample transfer arm system that is compatible with the option of automation. This design, while still in the conceptual phase was a great launching point for this project as it incorporates Maryland's existing design and takes it a step further by decreasing the height by a factor of three or four rather than two.

Additionally, this design allows for the necessary rotation and has the ability for automation of the sample transfer process.

2. Design

2.1. Design Specifications

The goals and design criteria that are used to evaluate designs and the final product are to:

a. Improve the resonance spectrum – Increase the resonant frequency by a factor of five to ten times the current manipulator resonant frequency.
b. Protect the STM head – Design a system that prevents damage to the critical STM head.
c. Maintain UHV Compatibility – The entire system should be UHV compatible to 10e-11 Torr.
d. Ensure the ability of the entire system to be heated to 150 C as an important step for establishing UHV conditions.
e. Incorporate Sample Movement – Design a system that incorporates the 360-degree rotation and shaft height adjustment of 2-5in. necessary for sample insertion and removal.

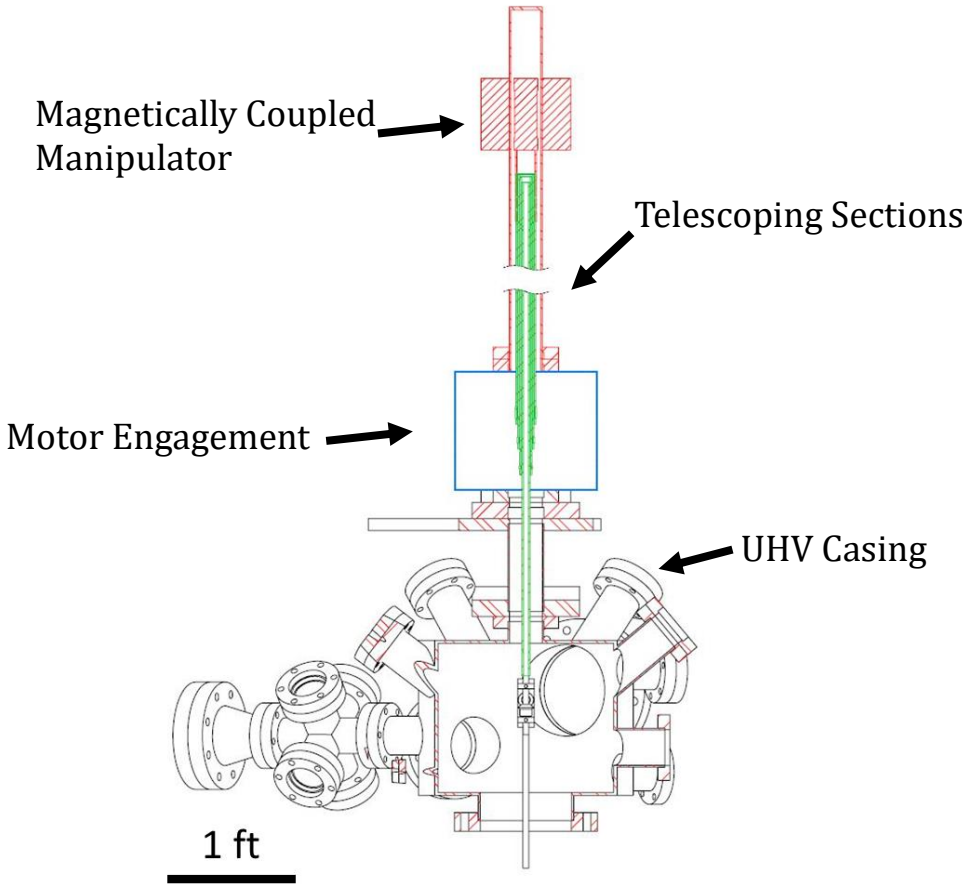

Figure 2: Cross-Section Component View of Compact Telescoping Sample Manipulator Design

2.2. Overall Design

The compact telescoping sample manipulator design can be categorized into four distinct sections, each with their own design specifications, specificities, and goals.

2.2.1. Telescoping Sections

The first major component of the design is the telescoping arm shown in Figure 2 in green and in a CAD model in Figure 3. The sections that make up the telescoping arm allow for the sample to be moved from the transfer chamber (Figure 1 (a)) down to the STM head. The sections need to telescope to an extended length of 73in. below the X/Y stage (Figure 1 (a)) to reach the STM head.

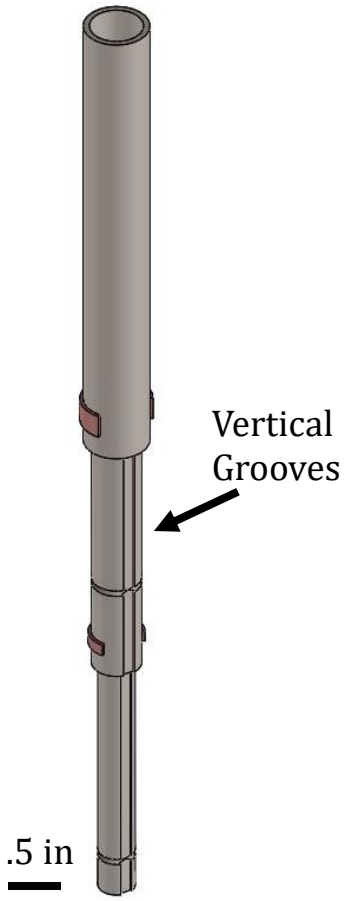

Figure 3: CAD Model of Telescoping Sections[1]

Figure 3 shows three telescoping sections and features two components to the telescoping section design. The first is the groove that runs vertically down the telescoping sections. These grooves, along with pins on the interior of the outer sections, allow for

[1] Figure 3 shows a prototype model with the correct diameters for the telescoping sections, while the lengths of the sections are shortened for presentation and prototyping purposes.

rotational coupling between the top stage and the bottom stage where the sample is attached. This provides control over the 360-degree rotation necessary for sample removal and insertion.

The second purpose of the vertical grooves is to provide a safety measure. The vertical grooves end at the fully extended position and therefore the sections cannot over extend and crash into the STM head[2].

The second featured component to the telescoping sections is the locking mechanism shown as a zoomed in cross section in Figure 4. The locking mechanism is comprised of copper beryllium (BeCu) C-shaped springs that push titanium ball bearings into slots that lie along the length of the telescoping sections. The copper beryllium springs are relaxed in the contracted position shown in Figure 4 and get pushed out when the titanium bearings are out of slots. This design allows the springs to lock in the ball bearings when the locking mechanism comes along a set of slots.

Beryllium copper (BeCu) is a good candidate for the material of the springs as it has a high flexure fatigue strength of 10e5 cycles to failure [5] and is commonly used in UHV environments for springs and electrical connections because of its retained elasticity at low temperatures. BeCu C17200 is the specific alloy used and has a composition of 1.9% Be, 98.1% Cu.

Titanium is also good material choice for the ball bearings as cold welding of like materials (i.e. stainless steel on stainless steel) is a concern in cold UHV environments. Therefore, the ball bearings must be not stainless steel while still maintain a low outgassing profile. Outgassing is an issue for vacuum systems in which if the vapor pressure of a material is higher than the vacuum that the material is in, it will sublime and become a vapor that could coat the sample surface. Since STM is a surface sensitive technique even singe atom contaminations on the surface would be detrimental to the measurements.

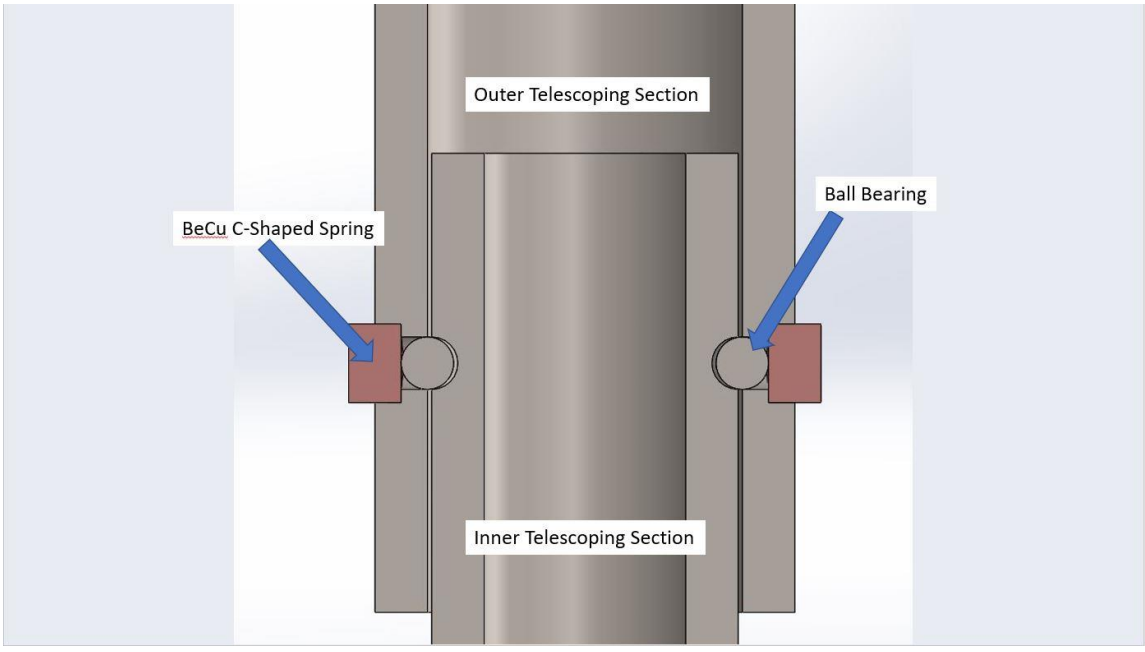

Figure 4: Zoom-in on cross section of telescoping joint locking mechanism**.** C-shaped BeCu springs push Ti bearings into grooves located on either end of the inner telescoping section.

[2] Further detailed drawings can be found in Appendix B

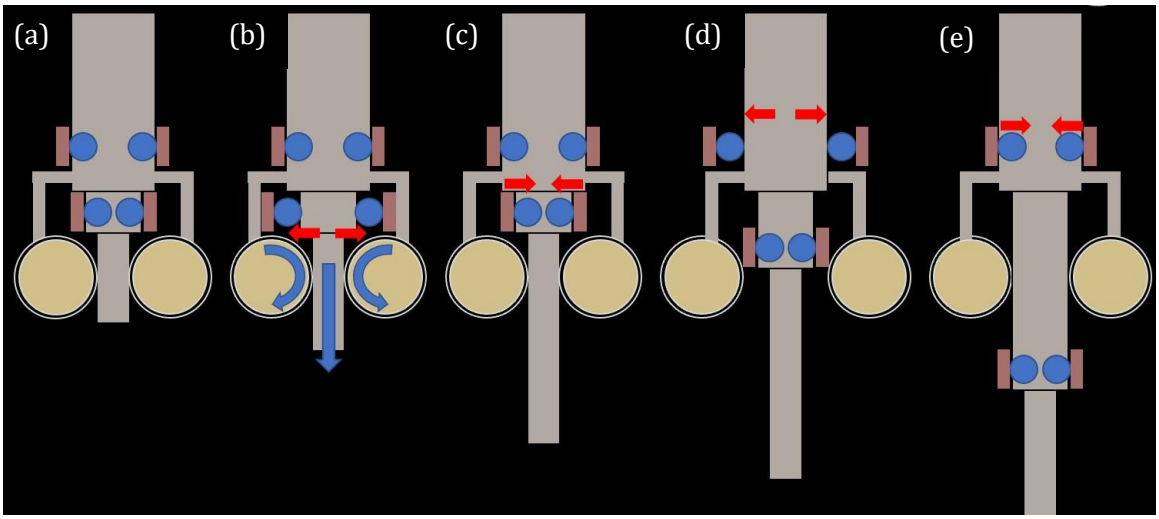

Figure 5: Step by step diagram of telescoping sections extension and retraction. **(a)** Fully retracted, **(b)** Motor engagement engages the smallest section down and unlocks the lower locking mechanism, **(c)** Lower locking mechanism locks in, pin engages vertical groove to limit extension, **(d)** Upper locking mechanism unlocks, **(e)** Upper locking mechanism locks in full extended position.

Figure 5 shows a more detailed walk through of the extension and retraction of the telescoping sections with the motor engagement simplified as schematic wheels. Starting from the fully compressed position (Figure 5 (a)), the motor engages with the first (smallest) section, unlocks the lowest spring (b), moves, and locks the first section into place (c). Then the motor engages with the second section (second smallest) unlocks (d), moves, and locks the second section (e). These steps can be repeated until the final section is locked into place and the arm is fully extended. This process can then be completed in the reverse to retract the arm and retrieve a sample from the STM head.

In step (b) it is critical that the lower locking mechanism unlocks while all the other sections stay locked. Previous work has been done with COMSOL simulations to show that the spring constants of the copper beryllium springs are dependent on the height of the spring (Appendix C). To ensure that the lower locking mechanism unlocks first the lower copper beryllium spring is shorter than the upper copper beryllium spring.

The locking mechanisms on the telescoping sections need to be able to lock and unlock each section in the correct order. They also need to make the telescoping manipulator rigid enough such that when fully extended the arm won't bend and miss the guide that is near the STM. In order to ensure that the manipulator hits the guide, the manipulator needs to be accurate to within +- 1mm when fully extended. The guide assists and lines up the end of the manipulator to insert a sample into the sample holder in the STM head.

Further design considerations of the telescoping section are that there are heat transferring baffles along the length of the path down to the STM head, that limit the diameter of the manipulator. The baffles have a hole in the middle that allows for a ½in. diameter shaft. The first baffle is 25 ⅞in. below the X\Y stage. Therefore, the telescoping sections can have a maximum diameter of ½in. 25 ⅞in. below the X/Y Stage.

In order to maintain the technical specification of UHV compatibility, stainless steel 304 is the chosen material for the telescoping sections as it has the properties of high strength as well as low outgassing and is readily available in a variety of sizes, which makes it an ideal candidate for this UHV application.

2.2.2. Motor Engagement

The second section of this project is the motor engagement and automation of the telescoping arm. Two options have been explored: a) an internal UHV-compatible motor and b) an external motor which is coupled to the manipulator via a rotary feedthrough. The comparable cost and questionable vacuum compatibility of an internal UHV motor drive outweighs the complexity of having an external motor drive. Therefore, an external motor drive was chosen.

A major roadblock of an external motor is the ability to transfer rotational power from the exterior non-vacuum environment to the interior vacuum environment while still allowing for linear and rotational freedom for fine adjustments as per the design specifications. The design shown in Figures 6 and 7 allow for the rotation of the telescoping section as well as the freedom for fine adjustments.

The u-joint, spline nut, and wobble stick combination shown in Figure 6 (a) allows for the ability to decouple the rotational energy coming from the external motor to allow the telescoping sections (shown as the grey circle) to rotate freely in order to insert and remove samples from the sample holder.

Further design considerations of the motor engagement design are that the motor needs engage with the telescoping manipulator to maintain control and contact with the arm to not drop the arm and damage the STM head. This is accomplished by implementing Viton O-rings as the interface to the telescoping sections. The rubbery texture of the Viton O-ring interfacing with the smooth stainless-steel telescoping sections along with the spring compressed contact (Figure 7) allow for control and contact with the telescoping sections. Viton rubber O-rings are UHV compatible after they are sufficiently heated and cleaned. Viton O-rings are commonly used in UHV systems as seals. The Viton O-rings are shown in Figure 6 (b) included with a PEEK cylinder.

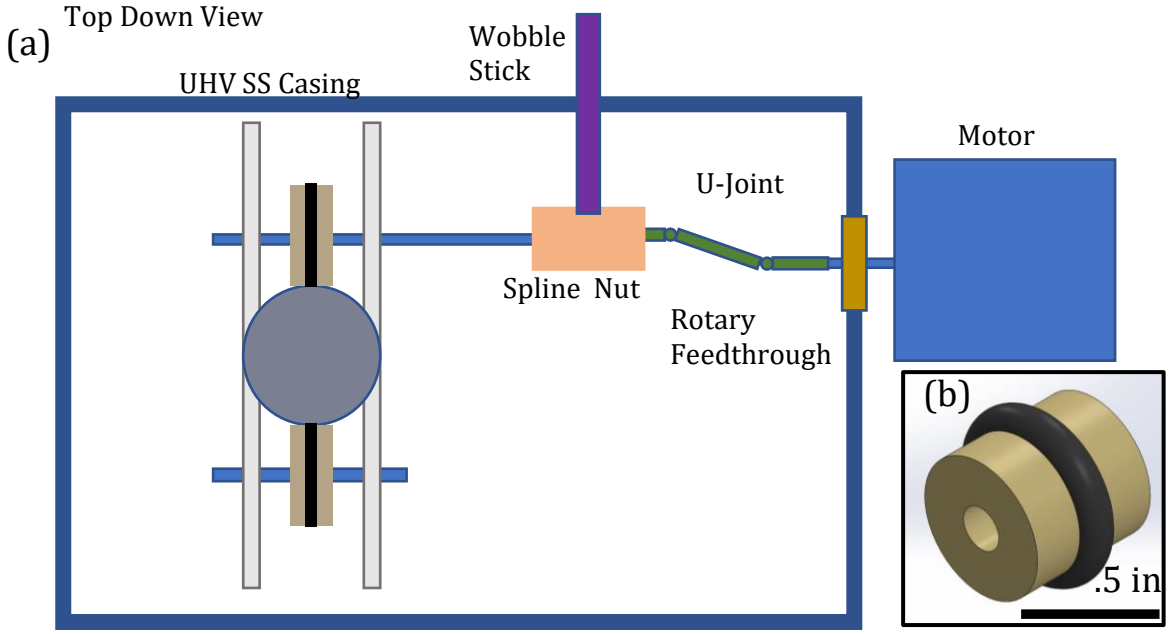

Figure 6: (a) Motor engagement top-down-view schematic, **(b)** Viton O-ring on PEEK cylinder

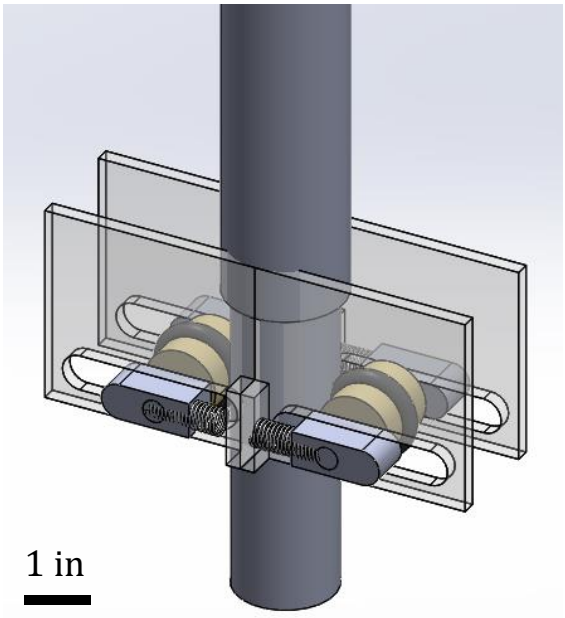

Figure 7: CAD model of motor engagement with Viton O-rings and a spring-loaded engagement

Because the motor engagement design has plenty of moving parts the system should be well lubricated. Lubrication is a large problem within UHV and further exploration is needed to find the correct lubrication for the motor engagement system to prevent seizing. Current lubrications that are used within the Hoffman Lab STM and other UHV systems include MoS_2 and Apiezon.

The motor engagement system in further iterations should also include a control system that includes sensors to detect if the arm is not on course, hits something, and when the arm is fully extended. In order to maintain UHV conditions the telescoping sections should be driven at a speed such that the arm fully extends in 4-5mins.

2.2.3. Magnetically Coupled Manipulator

The third component of the system design is the magnetically coupled manipulator (Figure 8(a)). This component is readily available to purchase with little customization and is a common component of UHV and STM systems.

The magnetic coupling presents a way to manually manipulate the telescoping transfer arm through the UHV casing. Magnetic couplings allow for a full 360-degree rotation and small height adjustments. These rotational and height adjustments are critical to inserting and removing a sample from the STM head. A magnetic coupling also allows for the sample to be inserted and removed with a human touch to get the force, feel, and responsiveness needed to carefully insert a sample into the STM head.

With this design the motor fully extends the telescoping sections and then the magnetic coupling allows for a lab member to rotate and insert the sample within the last 2-3in. The magnetic coupling of the magnet to the fourth telescoping stage allows for both adjustments.

Figure 8 shows the exterior and interior mechanism for a magnetic coupling. The inner rod shown in Figure 8 (b) is coupled to the exterior magnet shown in Figure 8 (a). A magnetic coupler also includes internal linear and rotational bearings (Figure 8(a)). The bearings are important in the ability for the telescoping arm to be dependably extended and retracted. The bearings also provide a tight fit near the base of the magnetically coupled manipulator to

prevent the telescoping sections from vibrating to a significant degree inside the magnetically coupled manipulator casing.

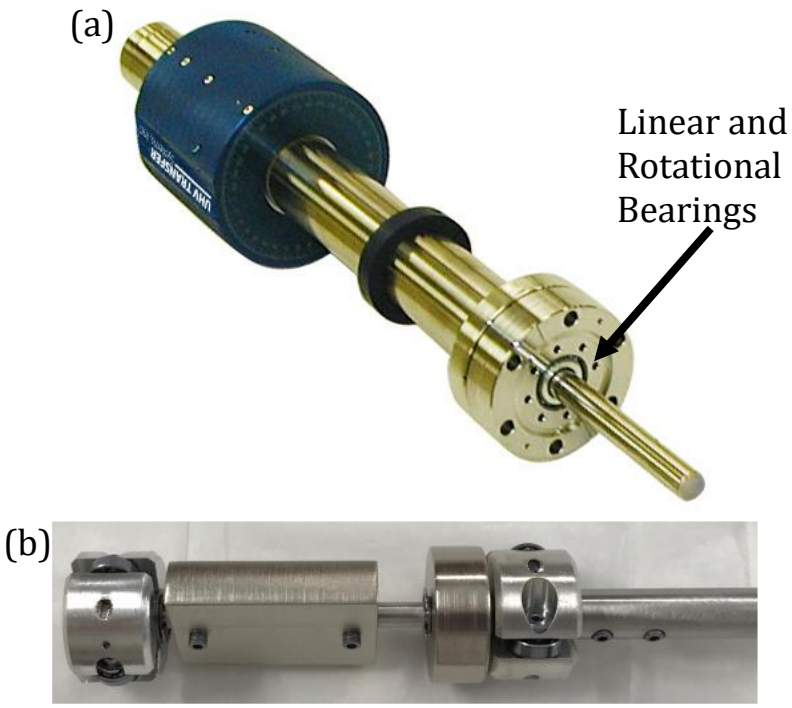

Figure 8: (a) Magnetic coupling arm from transfer engineering [6], **(b)** The interior assembly of a magnetic coupling arm[3]

The magnetic coupler will easily attach to the motor engagement chamber (Figure 1 (a)) through a UHV CF flange. The telescoping sections will be mounted to the bottom of the inner rod similar to Figure 8 (a).

2.2.4. UHV Casing

The final major section of this project is the UHV casing (Figure 2). The telescopic arm, motor engagement and magnetic coupling need to be surrounded by a casing that is compatible with the UHV conditions of the system. A typical UHV casing requires UHV welding and is constructed out of stainless steel for its vacuum compatible properties described in Section 2.2.1.

3. Builds and Iterations

The main section of the design that the build and iteration portion focus on is the critical module of the telescoping sections.[4]

[3] See Appendix B for more detailed drawings of the magnetically coupled manipulator
[4] The first three prototypes were built with a handheld scale in mind. The diameters of the telescoping sections are to scale, but the lengths of each section are reduced for ease of manufacturing and portability.

3.1. Prototype 1: 3-D Print

Figure 9: (a) 3_D Printed Prototype, extended with light green acrylic springs, **(b)** Zoom in on the acrylic springs

In order to obtain an intuition for the feasibility and scale of the telescoping sections, the first prototype was produced on a MakerGear M2 3-D printer with PLA filament that served as a proof of concept prototype. The 3-D prototype also served a presentation purpose in meetings and helped convey ideas in group meetings. The prototype extended and retracted and included acrylic springs, (Figure 9 (b)) but did not include the variable spring height to ensure that the arm would extend and retract in the correct order.

One of the conclusions from this prototype was that the surface finish of the material is critical. The surface finish is critical not only on the inner diameter but the outer diameter as well, to assure a smooth extension and retraction. Previously, a focus had been placed on the inner diameter smoothness while ignoring the matching interface of the outer diameter of the inside telescoping section.

3.2. Prototype 2: Metal Manufacturing

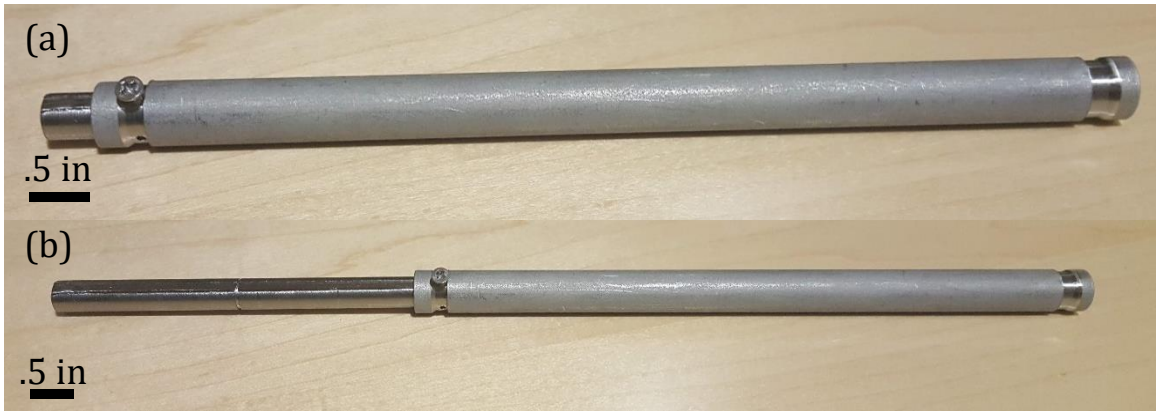

Figure 10: Stainless-steel 304 prototype **(a)** Retracted **(b)** Extended

The second prototype developed was made out of stainless steel 304. The purpose of the stainless-steel 304 protype was to practice the manufacturing techniques of the telescoping sections in the machine shop as well as get a more realistic sense of how the telescoping sections actuate. The stainless-steel 304 prototype extends and retracts but doesn't include any springs or bearings within the locking mechanism. One of the challenges faced in manufacturing this prototype was obtaining the correct tolerances needed to ensure a

smooth extension and retraction while not being too loose and lose the accuracy needed to hit the guide near the STM head during a sample insertion. Another challenge faced was the manufacturing of the pins that engage the vertical grooves shown in Figure 3. The pins were simplified to a set screw shown in Figure 10.

Similar to the 3-D printed prototype, surface finish was an issue in this prototype. Sanding and polishing of the exterior of the telescoping sections was not extensive enough as there was a rough extension and retraction of the telescoping sections. Prototypes 3 and 4 implemented more sanding and polishing of the exterior of the telescoping sections to obtain smoother surface finishes.

3.3. Prototype 3: Endpiece Design

One of the main manufacturing problems that was encountered in the previous prototypes was how to ensure a smooth bore on the inner diameter of the telescoping sections. To counter this manufacturing problem, an endpiece design was developed. The endpiece design allows for an accurately reamed inner diameter on a shorter length of tubing that acts at the interaction point between the inner and outer telescoping sections. Figure 11 (a)(b) shows a 3-D model of the design while Figure 11 (c)(d) shows the prototype that incorporated the endpiece design and allowed for smoother extension/retraction action. The endpiece is attached to the rest of the telescoping section by UHV compatible glue, Varian Torr Seal, that is currently used in the Hoffman Lab STM system.

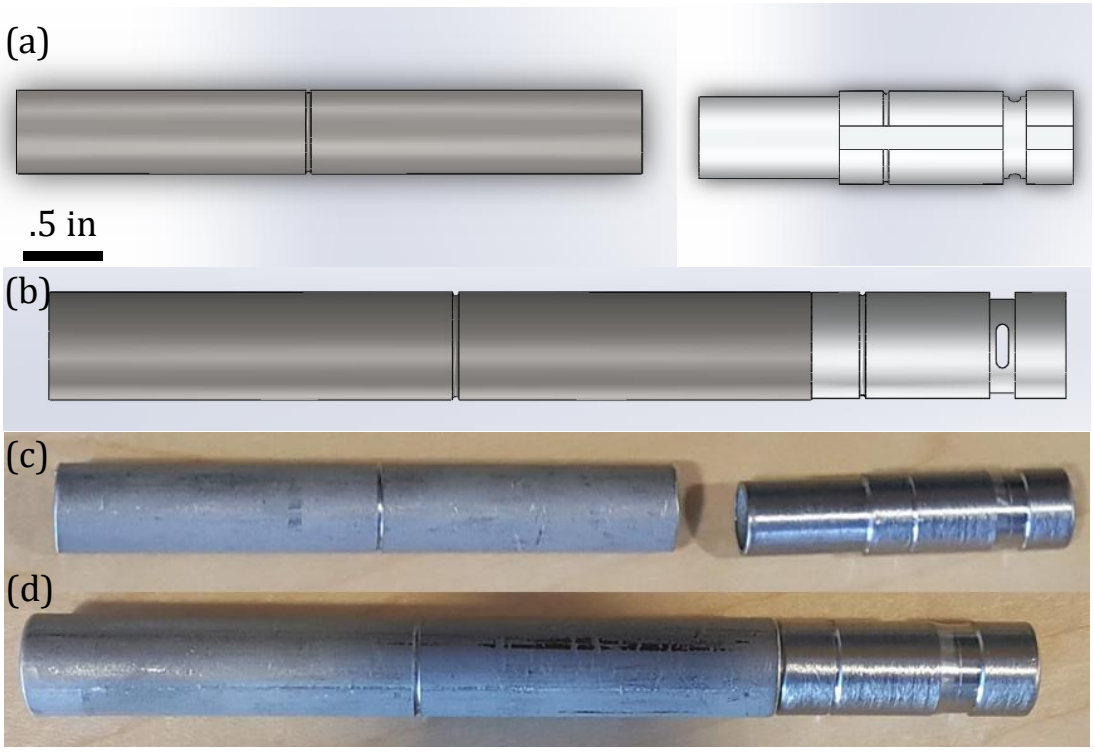

Figure 11: (a)(b) CAD endpiece assembly model **(c)(d)** Stainless-steel 304 prototype with endpiece design

Springs made out of a BeCu thin sheet were made for this prototype as well. The 0.0175 in. thick BeCu sheet was cut into thin strips and then bent around stainless-steel tubes to obtain the correct diameter. This resulted in C-shaped springs. However, one of the problems was that the springs were very malleable and didn't maintain their shape after a couple of cycles, making them not useful.

3.4. Prototype 4: Full Scale

The final prototype was a full-scale prototype manufactured out of stainless steel 304 with a PEEK endpiece incorporated shown in Figure 12. PEEK was chosen for the endpiece material due to its UHV compatibility and reduced coefficient of friction. This prototype ran into an assortment of manufacturing issues due to the increase in length of the telescoping section.

The first problem encountered was trying to turn down the outer diameter of the telescoping sections to the correct diameter on the lathe. The long stainless-steel tube deflected enough under the forces of turning down the diameter that it led to an uneven exterior finish along the length of the shaft. To counteract this problem, all of the turning down of the tube needed to be done close enough to the headstock of the lathe that the tube didn't deflect creating the uneven surface. This led to the time-consuming process of turning down ~2in. of the tube and then shifting down the tube away from the headstock to turn down the next ~2in. for the length of the tube.

Another problem encountered was deflection when attempting to implement the vertical grooves shown in Figure 3. On the previous shorter, scaled-down prototypes clamping the tube in the mill vise provided sufficient stability for milling the groove along the length of the entire tube. When the telescoping section was scaled up in this prototype, clamping the telescoping section in the vise was not sufficient clamping as the lengths hanging off the edges of the vise deflected similar to on the lathe and caused an uneven depth of groove along the telescoping section. This deflection combined with the narrowness of the groove, lead to breaking the endmill used to cut the groove.

The final problem in the manufacturing of this prototype was that the UHV glue used, Varian Torr Seal, expanded when it dried. The tolerances of the telescoping sections provided a smooth extension and retraction when dry fitted together. Then after gluing and the glue expanded, the PEEK endpiece became too tight to allow for smooth extension and retraction.

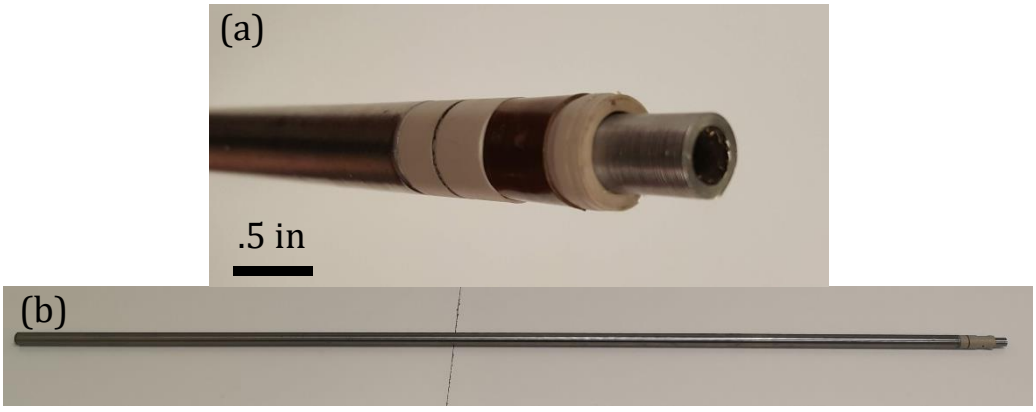

Figure 12: (a) Zoom in of the PEEK endpice and BeCu spring, **(b)** Overall view of final full-scale prototype 32in. in length

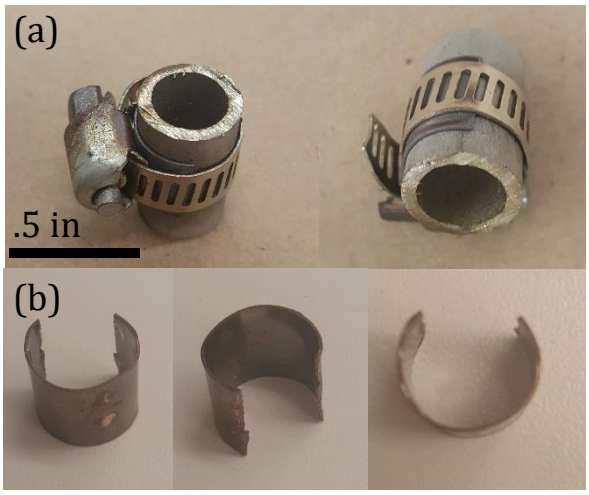

Figure 13: (a) BeCu springs being formed with hose clamps, **(b)** Final form of annealed BeCu springs

To improve the BeCu springs from previous prototypes and make the springs more ridged the springs were subject to an annealing process. The springs were formed using stainless-steel tubing and hose clamps as shown in Figure 13 (a). Then the springs were heated to anneal the BeCu in order to reset the internal strains and stresses of the material to make the C-shape the relaxed and original position. Therefore, when the springs were expanded during operation, the springs maintained pressure and to returned to the locked position as designed. The BeCu springs were annealed at 315 C for 3 hrs.[5]. [5]. One of the downsides to the annealing process is that the springs oxidized while annealing and would require additional cleaning to become UHV compatible (Figure 13 (b)). Cleaning or annealing in an atmosphere of inert gas (e.g. Argon) in a tube furnace would both reduce the oxidization.

4. Tests and Measurements

4.1. Test Objectives

The main project specification that was tested was to:

a. Improve the resonance spectrum – Increase the resonant frequency by a factor of five to ten times the current manipulator resonant frequency.

4.2. Test Set Up

In order to test the final full-scale prototype, a test rig was designed and built to attach the telescoping sections to the STM table. A testing rig mounted on the table replaces the lengthy process of installation of the manipulator, which can take up to three months of installation troubleshooting with a commercial sample manipulator turned out to be out of the scope of this project.

[5] More information on the annealing characteristics can be found in Appendix (C.1)

The testing set up is a box frame constructed out of 80/20 aluminum structural framing and is 4in. x 6in. x 6in. (Figure 14 (1)). The frame is mounted to the table to simulate the UHV casing of the motor engagement (Figure 2). On the top of the 80/20 box frame is a water-jet piece of aluminum to meld the box frame to the pipe flange bracket. Along with the water-jet piece of aluminum is a machined piece of aluminum with a tight-fitting hole that acts as the set of bearings that would be attached to the bottom of the magnetically coupled manipulator (Section 2.2.3.) (Figure 14 (2)). On top of the water-jet aluminum and synthetic bearing, the pipe flange bracket (Figure 14 (3)) mounts to a steel pipe that encases and acts as the UHV casing on the magnetically coupled manipulator (Figure 14 (4)). The telescoping sections are held in the steep pipe by a series of bolts that allow for adjustment of the sample and ease of access and inssertion of the telescoping sections. (Figure 14 (5)).

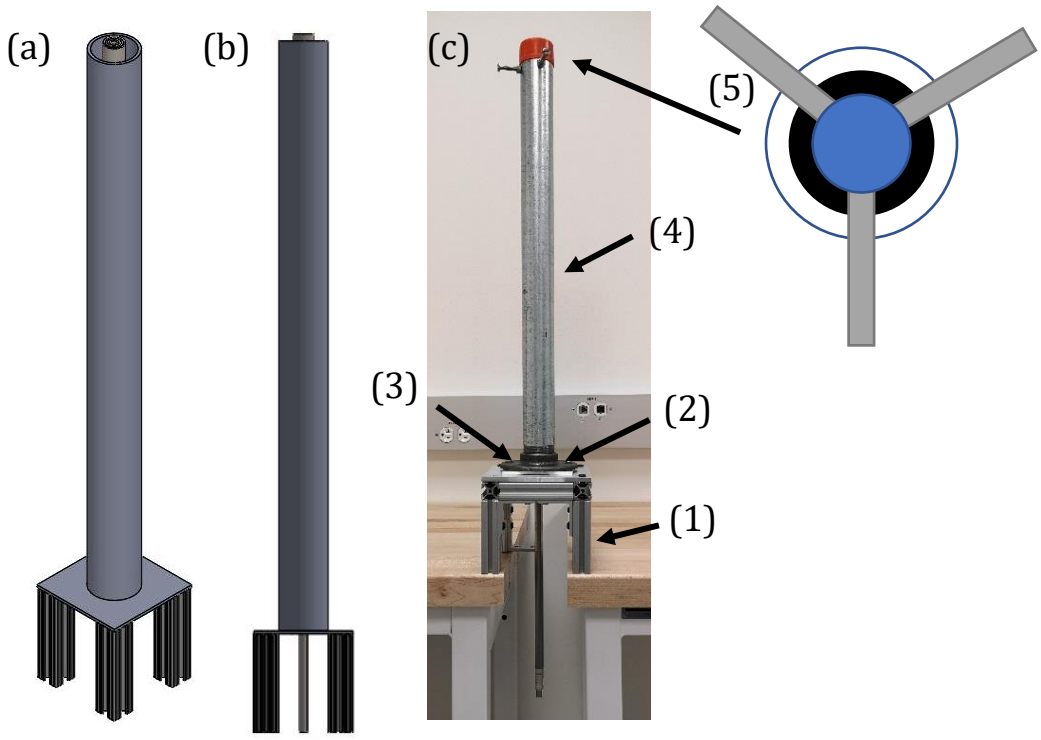

Figure 14: (a)(b) CAD model of testing rig**, (c)** Built test rig with telescoping sections installed **(1)** 80/30 aluminum base **(2)** Water-jet Aluminum bracket and bearing **(3)** Pipe flange bracket **(4)** Steel pipe **(5)** Telescoping section mounting top-down schematic

4.3. Vibration Spectrum Test of Current Manipulator

To further motivate the project and a control of the current sample manipulator's effect on the vibrational spectrum of the STM system was obtained with the results shown in Figure 15.

The vibration data was measured using a geophone that sits near the STM head (Figure 16). A baseline (system at rest) spectrum at optimized measurement conditions was obtained over a time period of ~8hrs. To obtain the vibration spectrum of the currently installed long manipulator (system excited) string was attached with scotch tape to the top of the current sample manipulator and pulled off. This external force excited the sample manipulator and caused it to oscillate back and forth (Figure 16). The Table resonance is shown at 1.5Hz while the manipulator resonates at 3Hz.

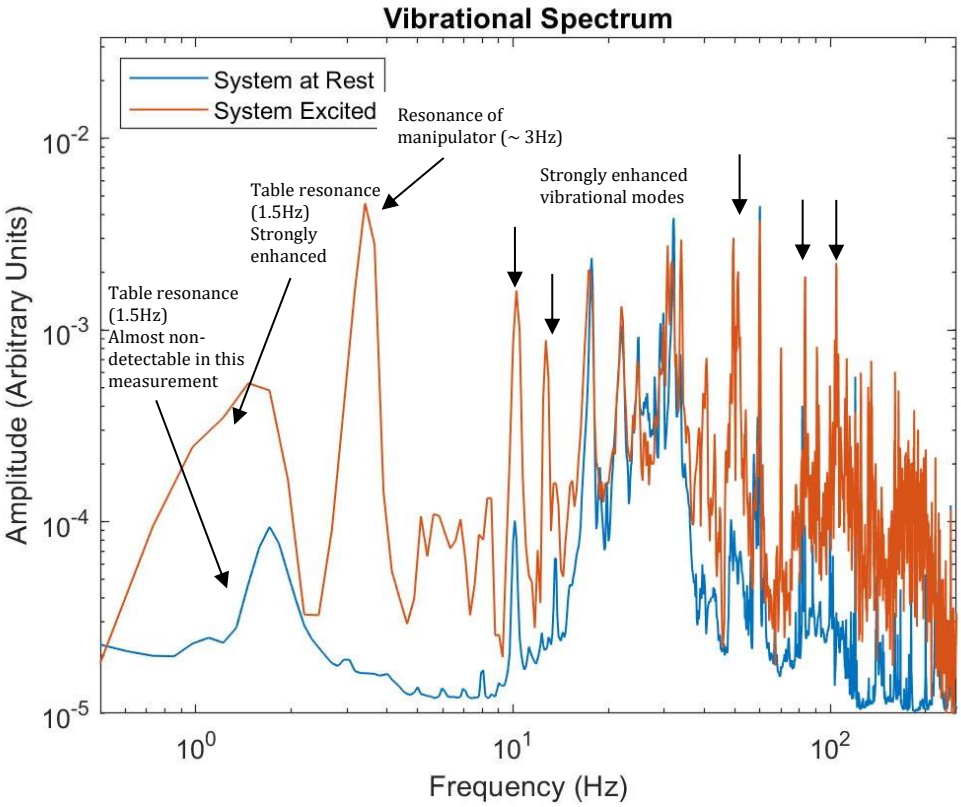

Figure 15: Vibrational Spectrum of current manipulator

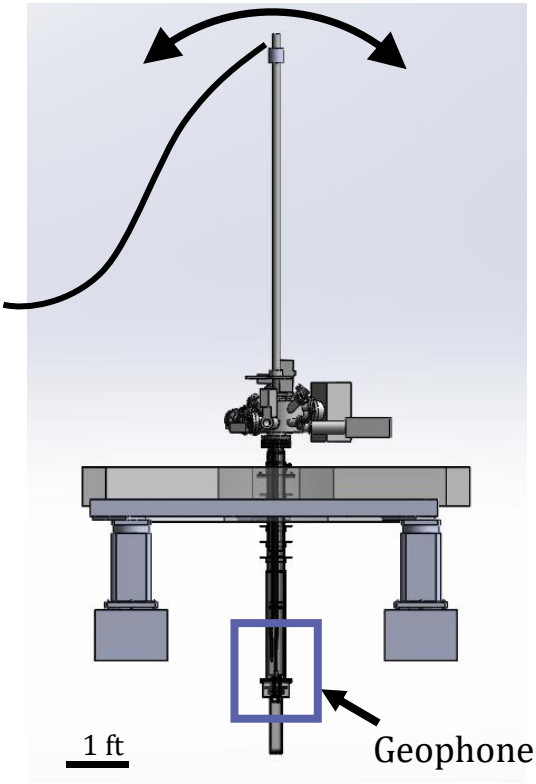

Figure 16: Experimental setup to obtain vibrational spectrum

This test concludes that: (1) the magnitudes of the ambient vibrations from the existing sample manipulator are large enough that they are reaching and affecting the STM head and (2) when the current sample manipulator is excited, it couples to the main resonance of the table, disturbing the isolation system and exciting many frequency modes of other components in the STM system.

4.4. Vibration Spectrum Test

In order to test the effect of the telescoping manipulator on the STM system a similar test to the baseline vibration spectrum test was performed with the test rig and telescoping full-scale prototype mounted on the table. [6] Vibration data for the test was collected from both a geophone close to the STM as in the previous test as well as another geophone placed on the table itself.

The vibration test was performed in a similar way as the previous measurement. The baseline (system at rest) was again obtained by averaging the vibrational spectrum over an extended time (1-2 mins). The excited condition was obtained by tapping the testing rig with a rubber mallet and collecting the vibration data for ~1 min. after the excitation. Figure 17 shows the results of this test with the resonant frequency of the manipulator showing up at 20 Hz.

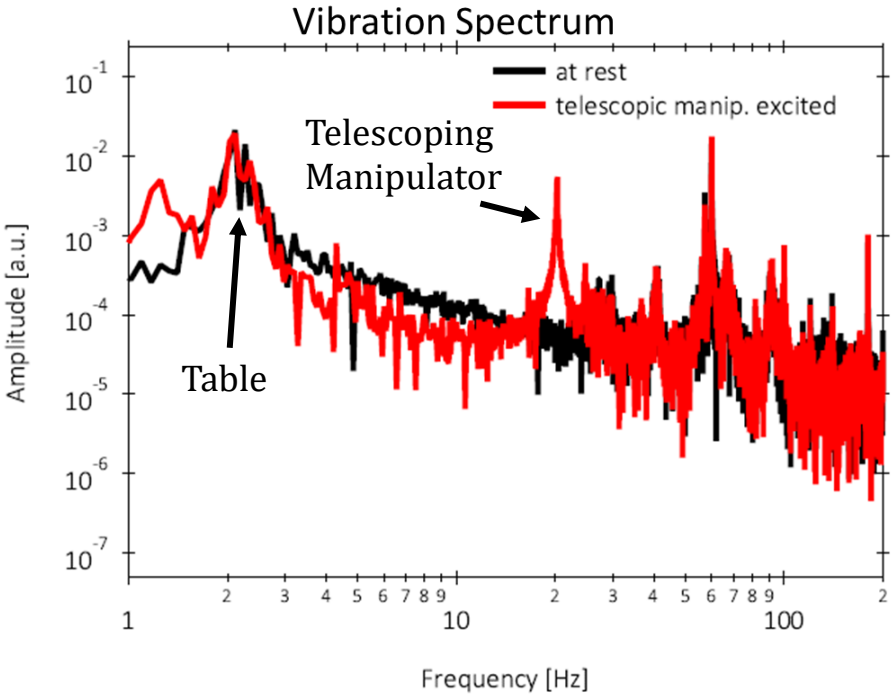

Figure 17: Vibration spectrum with telescoping manipulator prototype

This test also hints at a sharper resonance for the telescoping manipulator. Visually, the telescoping manipulator resonant frequency peak in Figure 17 is narrower than the existing manipulator's resonant frequency peak in Figure 15. Furthermore, the coupling to the table

[6] For logistical reasons the STM system that the vibration spectrum test and vibration spectrum movement tests are on is different than that of the baseline vibration test.

in Figure 17 is almost non-existent. More rigorous calculations of Q factors are needed to confirm these observations.

4.5. Vibration Spectrum Movement Test

To double check that the 20 Hz resonant frequency peak is the correct resonant frequency for the telescoping manipulator a second test was performed where the telescoping section was extended to five increasing heights. The telescoping section was extended from a fully retracted position to an almost fully extended length. It is expected with the variable heights that the resonant frequency peak should shift to lower resonant frequencies as the height of the telescoping manipulator is increased. Figure 18 shows the results of the test.

This test concludes that the resonant frequency that we identified in the previous test is indeed the resonant frequency of the telescoping manipulator. This test also shows an odd pattern of the 32Hz resonant frequency shows up on each height of the telescoping manipulator. One explination is that the test rig has its own resonant frequency 32Hz while the telescoping manipulator resonant frequency decreases as the height increases as expect separate from the test rig as shown in Figure 18 (b).

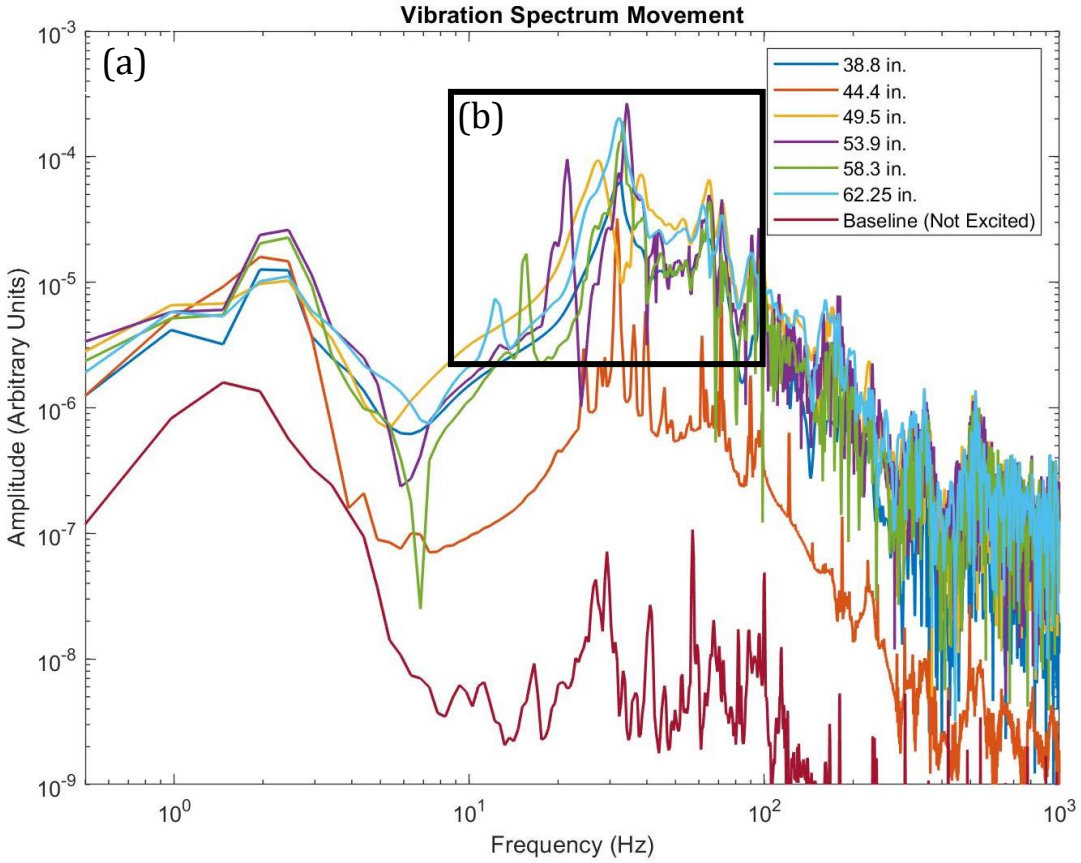

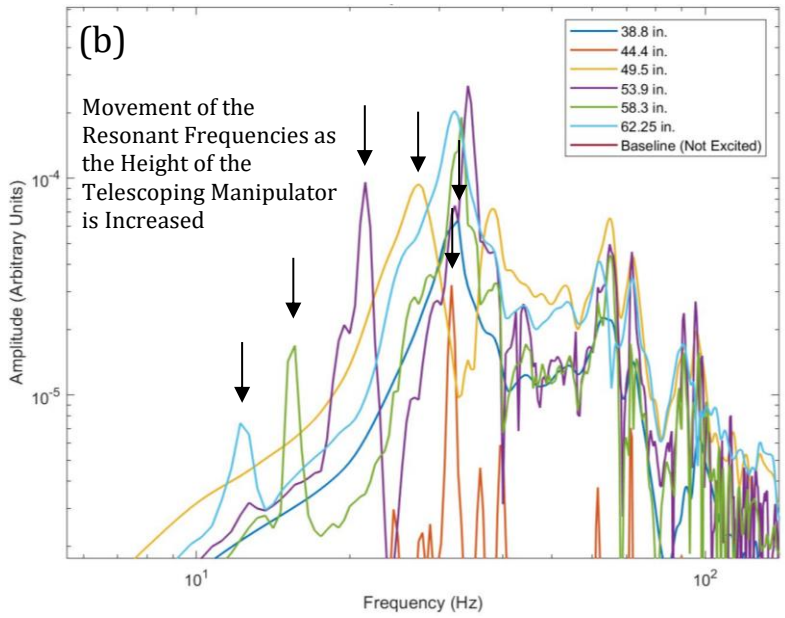

Figure 18: (a) Vibration spectrum movement test results **(b)** Zoom in of resonant frequency movement

5. Analysis

The results of the testing compared to the initial design specification indicate that the telescoping manipulator is successful in many aspects but failed to fully meet several specifications.

a. Improve the resonance spectrum – Increase the resonant frequency by a factor of five to ten times the current manipulator resonant frequency.

*insert gaussian fit calculations and the actual resonant peaks and then the change factor. * also highlight the fact that the plot shows that we have decoupled the manipulator from the table.

b. Protect the STM head – Design a system that prevents damage to the critical STM head.

Protection of the STM head is achieved through the vertical grooves that run the length of the telescoping sections and the pin counterparts that engage the grooves. Further work can be done to include an electromagnetic lock within the sensing and control system of the motor engagement design as an added protection measure to protect the STM head.

c. Maintain UHV Compatibility – The entire system should be UHV compatible to 10e-11 Torr.
d. Ensure the ability of the entire system to be heated to 150 C as an important step for establishing UHV conditions.

Both UHV compatibility and the ability of the entire system to be heated to 150 C are accomplished in the presented design through the selected materials. All materials used in

the design are either in current use within a Hoffman Lab STM system or on the approved list of materials for LIGO [7].

e. Incorporate Sample Movement – Design a system that incorporates the 360-degree rotation and shaft height adjustment of 2-5in. necessary for sample insertion and removal.

Sample Movement with the ability to rotate 360-degrees and have a shaft height adjustment of 2-5in. is accomplished in the presented design and specifically in the motor engagement design and the use of the magnetically coupled manipulator.

6. Conclusion

6.1. Conclusion

Scanning tunneling microscopes (STMs) can resolve the real space morphology and electronic structure of a crystal surface at atomic length scales. In order to achieve such high precision measurements, the stability of the instrument is a key factor and the effect of external disturbances has to be minimized. Many STMs require a long manipulator of 5 – 6 ft. in length that act as an antenna for acoustical and vibrational noise, disrupting atomic resolution imaging.

This project proposed a design for a telescoping manipulator system that reduces the length of the manipulator to 31 in. Through prototyping and testing it is shown that the telescoping design increases the resonant frequency of the manipulator from 3 Hz to 20 Hz for an increase by a factor of 6.6.

6.2. Future Work

Future work on this project includes expanding out and building on other portions of the design.

One area of improvement would be to improve or outsource the manufacturing processes. Most of the major roadblocks were encountered in the manufacturing of the full-scale prototype as discussed in Section 3.4. A lot of these issues could be avoided through better shop machines (lathes, mills, etc.), or outsourcing the manufacturing to a professional service.

Future work could be done to improve the pin installation which was simplified to a set screw design in this project's prototypes. One possible solution is to weld a pin in place and then make the tube concentric and 'clean up' the weld on the lathe. This solution would still be difficult as the lathe 'cleaning up' may compromise the structural integrity of the weld and make it useless.

Another simple improvement on the next iteration would be to redesign the tolerances of the telescoping sections to account for the UHV compatible glue's expansion when it dries or simply ream out the tube after the endpiece as been glued in place.

An expansion to design and implement a motor control system could be done within the motor engagement design. This control system should incorporate some sort of sensing and additional safety measures, including an electromechanical lock that would stop the motor and the lock the telescoping sections if the system senses that the telescoping sections are falling.

Finally, to further improve the vibration reduction portion of this project. The telescoping sections could be designed for a five or six stage system instead of the here proposed four stage system. By adding more stages, the telescoping manipulator could be shorter and further increase the resonant frequency of the manipulator.

Acknowledgements

I would like to first and foremost thank my faculty advisors, Jennifer Hoffman and Christian Matt, for being great mentors throughout this project. Without their help and guidance this project wouldn't be where it is today.

I'd like to thank Mohammad H. Hamidian for the inspiration and idea for this project as well as the rest of the Hoffman Lab for being supportive and providing critical feedback at group meetings and during presentations.

This project wouldn't have been possible without the ALL staff and their continued support throughout this project and being there to bounce ideas off of and suggest creative solutions to roadblocks.

I'd also like to thank the ES 100 teaching staff for the structure and organization of this course that made all of the ES 100 projects such a success. Including, Nishant Sule and his ES 100 section for being an open community to present and talk about the project and ideas.

I would like to thank Stan Cortreu and Steve Sansone for their patience and guidance in the machine shop through the manufacturing portion of this project.

Moreover, I'd like to thank my friends and ES 100 peers for also being an open ear for this project and creating such a collaborative environment within the ES 100 class.

Finally, I would like to thank my family for supporting me and inspiring me to shoot for the stars because a backup plan takes an afternoon to figure out.

References

[1] Roychowdury, Anita, M. A. Gubrud, R. Dana, J. R. Anderson, C. J. Lobb, F. C. Wellstood, and M. Dreyer. 2014. "A 30mK, 13.5 T Scanning Tunneling Microscope with Two Independent Tips." Review of Scientific Instruments 85, 043706: doi: 10.1063/1.4871056

[2] MacLeod, B. P., J. E. Hoffman, S. A. Burke, and D. A. Bonn. 2016. "Acoustic Buffeting by Infrasound in a Low Vibration Facility." Review of Scientific Instruments 87 (9) (September): 093901. doi: 10.1063/1.4962241

[3] Pabbi, L., A. R. Binion, R. Banerjee, B. Dusch, C. B. Shoop, and E. W. Hudson. 2018. "ANITA – An Active Vibration Cancellation System for Scanning Probe Microscopy." Review of Scientific Instruments 89, 063703: doi: 10.1063/1.5033457

[4] "LTTA – Linear Telescopic Transfer Arm." *LTTA – Linear Telescopic Transfer Arm,* https://www.lesker.com/newweb/sample_manipulation/linear-telescopic-transfer-arm.cfm

[5] Brush Wellman. Inc. *Guide to Copper Beryllium*. *Guide to Copper Beryllium*, Brush Wellman Inc., 2002.

[6] "PMM-Lite, Precision Magnetic Manipulator with Linear and Rotary Motion." *PMM-Lite Precision Magnetic Manipulator with Linear & Rotary Motion*, uhvtransfer.com/magnetic_PMM-lite.php

[7] Coyne, D. "LIGO Vacuum Compatible Materials List." 2014.

Appendices

A. Bill of Materials

This project has a difference between the bill of materials for the presented design and the bill of materials for the prototyping and development. Everything included in the prototyping and development was purchased and used in this project.

Prototyping and Development

BOM (Bill of Materials)	Unit Cost $	Unit	# of Units	Total $
Mirror-Like 304 Stainless Steel Round Tube 0.065" Wall Thickness, 1/2" OD	16.92	20 pack	1	16.92
304 Stainless Steel Round Tube, 0.12" Wall Thickness, 1/2" OD	17.32	1ft	1	17.32
G10/FR-4 GLASS EPOXY ROD, NATURAL, (0.500 IN X 4 FT)	32.9	1	1	32.9
Smooth-Bore Seamless 304 Stainless Steel Tubing 1/2" OD, 0.065" Wall Thickness	11.17	8 in	1	11.17
Smooth-Bore Seamless 304 Stainless Steel Tubing 3/8" OD, 0.065" Wall Thickness	9.95	8 in	1	9.95
Chemical-Resistant Viton® Fluoroelastomer O-Ring 3/16 Fractional Width, Dash Number 312	7.21	10 pack	1	7.21
Chemical-Resistant Viton® Fluoroelastomer O-Ring Square-Profile, 1/8 Fractional Width, Dash No. 210	7.27	5 pack	1	7.27
Oil-Resistant Soft Buna-N O-Rings 1/8 Fractional Width, Dash Number 210	10.65	50 pack	1	10.65
Smooth-Bore Seamless 304 Stainless Steel Tubing 1/2" OD, 0.065" Wall Thickness	22.34	8 in	2	11.17
Smooth-Bore Seamless 304 Stainless Steel Tubing 3/8" OD, 0.065" Wall Thickness	19.9	8 in	2	9.95
SS 304 Tubing 3/8" 0.065" Wall Thickness	25.31	3 ft	1	25.31
SS 304 Tubing 1/2" 0.065" Wall Thickness	29.96	3 ft	1	29.96
SS 304 Tubing 5/8" 0.065" Wall Thickness	36.44	3 ft	1	36.44
SS 304 Tubing 3/8" 0.065" Wall Thickness	38.62	3 ft	1	38.62

PEEK Rod Beige 1-1/2" Diameter	48.57	3 in	1	48.57
Titanium Ball Bearing 1/16" Diameter	28.13	5 pack	4	112.52
Uncoated Carbide Square-End End Mill 4 Flute,1/16" Mill Diameter, 1-1/2" Overall Length	12.84	1	1	12.84
Uncoated Carbide Square-End End Mill 4 Flute, 7/64" Mill Diameter, 1-1/2" Overall Length	12.06	1	1	12.06
1-1/2" x 2 ft. Galvanized Carbon Steel Nipple, Pipe Schedule 40	25.37	1	1	25.37
Floor Flange, Flanged x FNPT, 1-1/2" Pipe Size - Pipe Fitting	14.86	1	1	14.86
Brass Stock 1" Round	7	6 in	1	7
Aluminum Stock 4" x 4" x 1/4"	5	1	1	5
Waterjet Aluminum Plate	50	1	1	50
MakerGear PLA 3D Printing Filament	15	15 cm^3	1	15
1 in Square Aluminum 80/20 Framing	30	2 ft	1	30
Miscellaneous 1/4-20 Nuts and Bolts	2	10	1	2
80/20 Brackets and Bolts	2	10	1	2
				Total
				602.06

Table A.1: Prototyping and Development Bill of Materials

Presented Design

BOM (Bill of Materials)	Unit Cost $	Unit	# of Units	Total $
Telescoping Sections				
SS 304 Tubing 3/8" 0.065" Wall Thickness	25.31	3 ft	1	25.31
SS 304 Tubing 1/2" 0.065" Wall Thickness	29.96	3 ft	1	29.96
SS 304 Tubing 5/8" 0.065" Wall Thickness	36.44	3 ft	1	36.44
SS 304 Tubing 3/8" 0.065" Wall Thickness	38.62	3 ft	1	38.62
Locking Mechanism				
Springs 1" Round C17200 BeCu	169	6 in	1	169
PEEK Rod Beige 1-1/2" Diameter	48.57	3 in	1	48.57
Titanium Ball Bearing 1/16" Diameter	28.13	5 pack	4	112.52
UHV Casing				
Custom UHV Weld	500	1	1	500
Custom Manipulator	3200	1	1	3200

Custom Motor Engagement Casing	1000	1	1	1000
Motor Engagement				
O-Rings	7.21	10 pack	1	7.21
Electro-Magnetic Lock	500	1	1	500
Wobble Stick	2450	1	1	2450
Linear Bearings for Spline Shaft 10mm	74.61	1	1	74.61
Spine Shaft 10mm Diameter	97.99	200 mm	1	97.99
U-Joint Machinable-Bore Double U-Joint	120.03	1	1	120.03
Rotational Feedthrough	500	1	1	500
External Motor	200	1	1	200
				Total
				9110.26

Table A.2: Presented Design Bill of Materials

B. Engineering Drawings

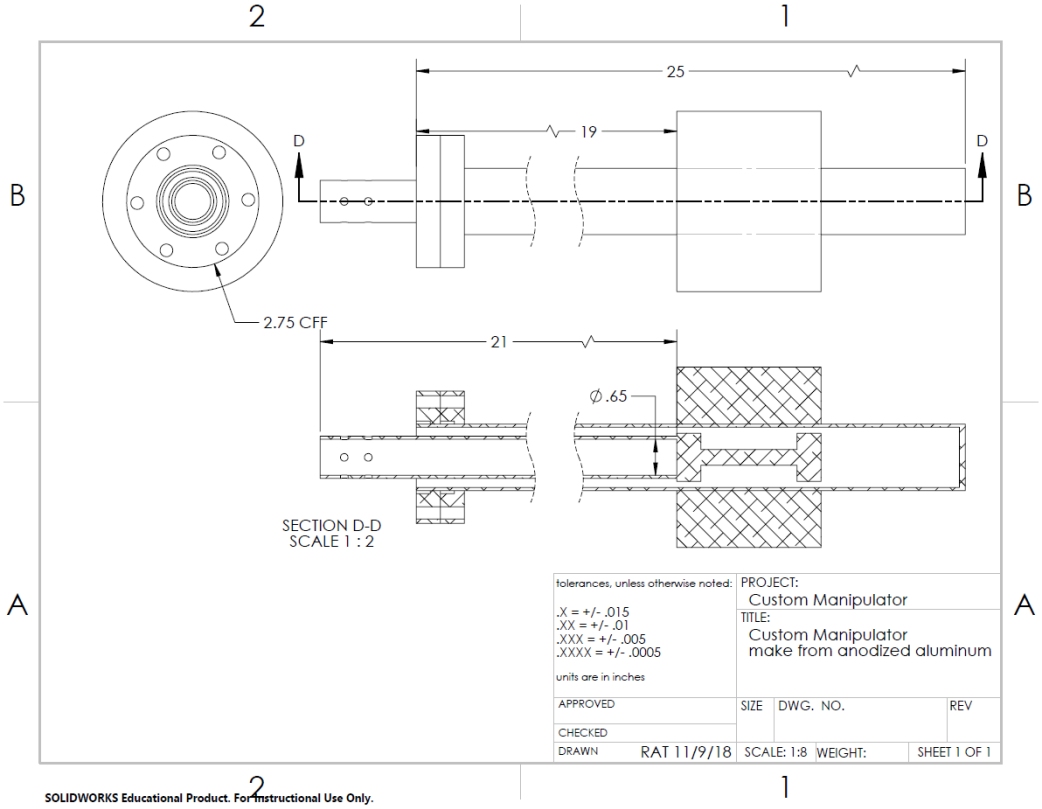

Figure B-1: Magnetic manipulator designed for the telescoping manipulator

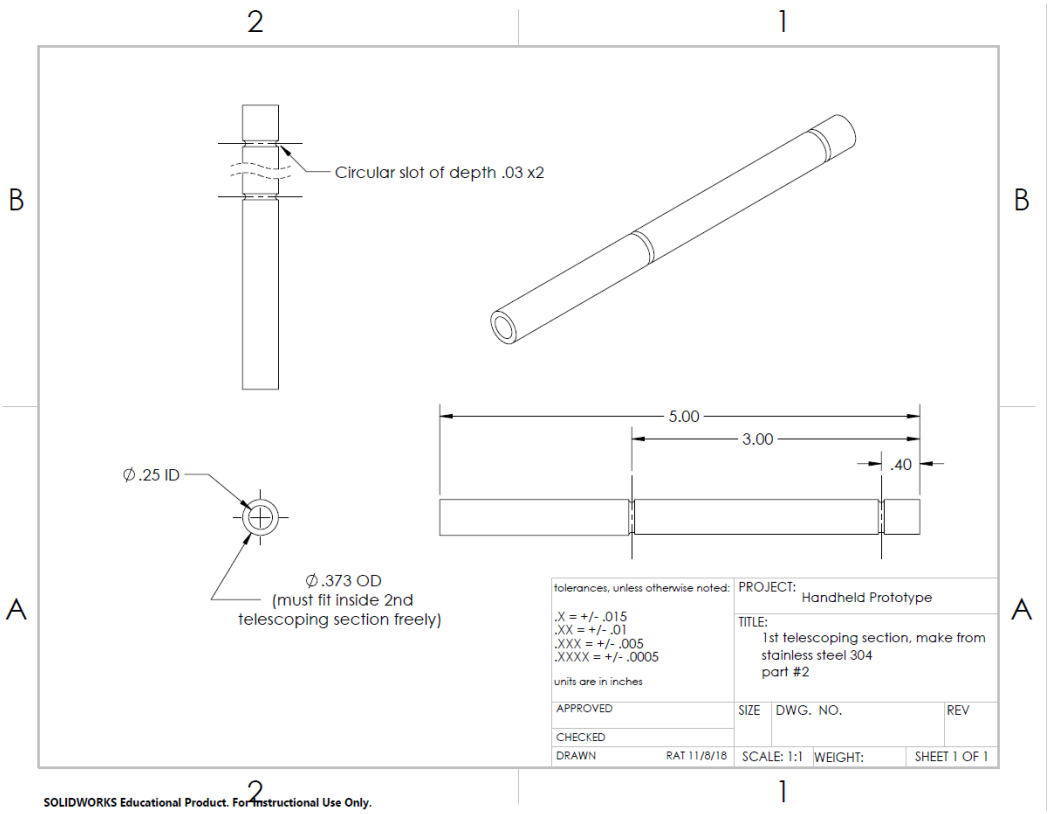

Figure B-2: Inner telescoping section for prototype 2: metal manufacturing

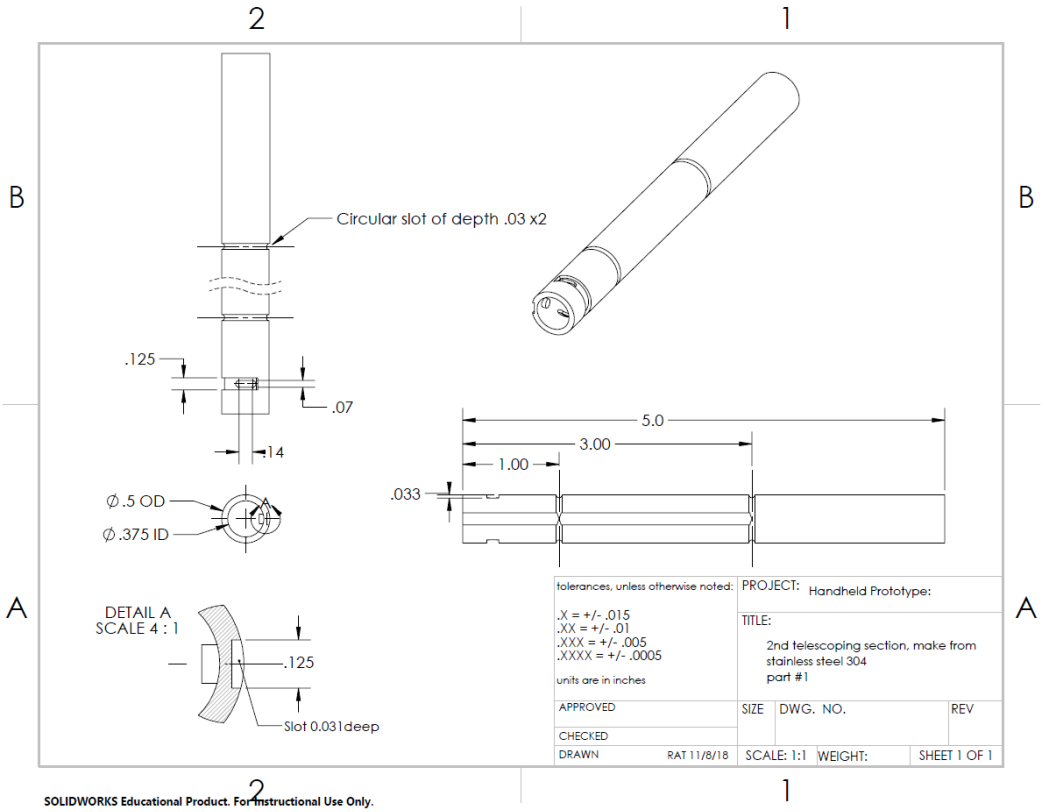

Figure B-3: Outer telescoping section for prototype 2: Metal manufacturing

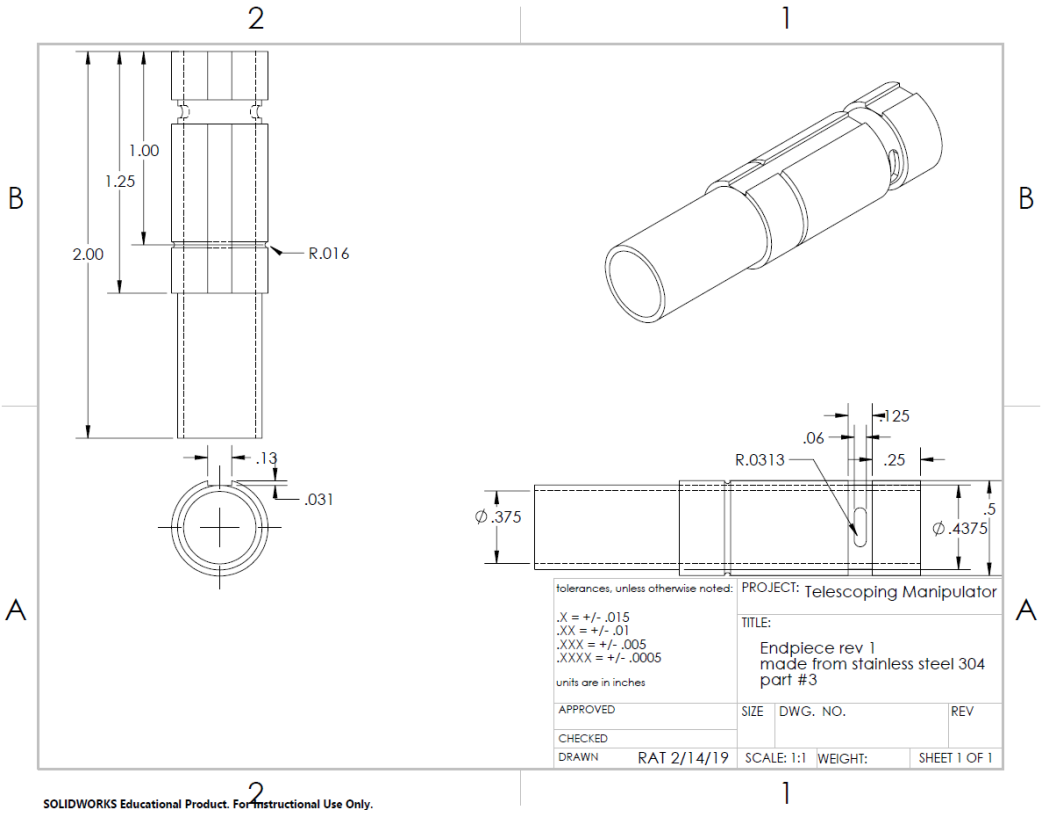

Figure B-3: Endpiece design for prototype 3: endpiece design

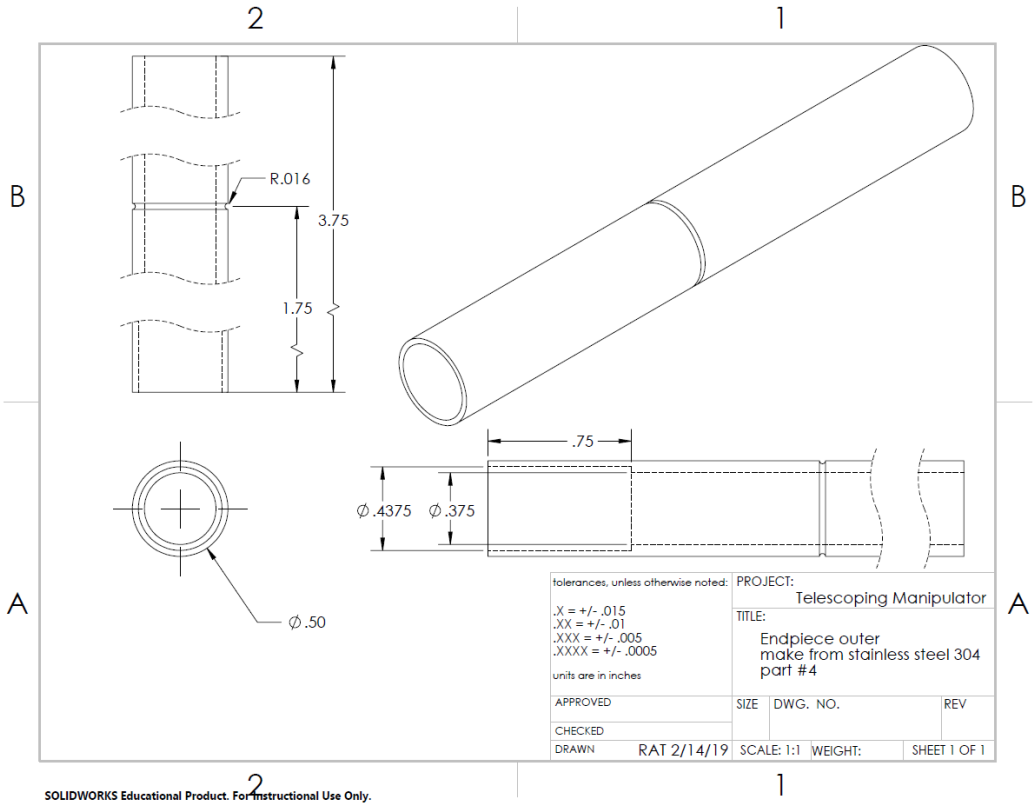

Figure B-4: Female telescoping section to meld to the endpiece for prototype 3: endpiece design

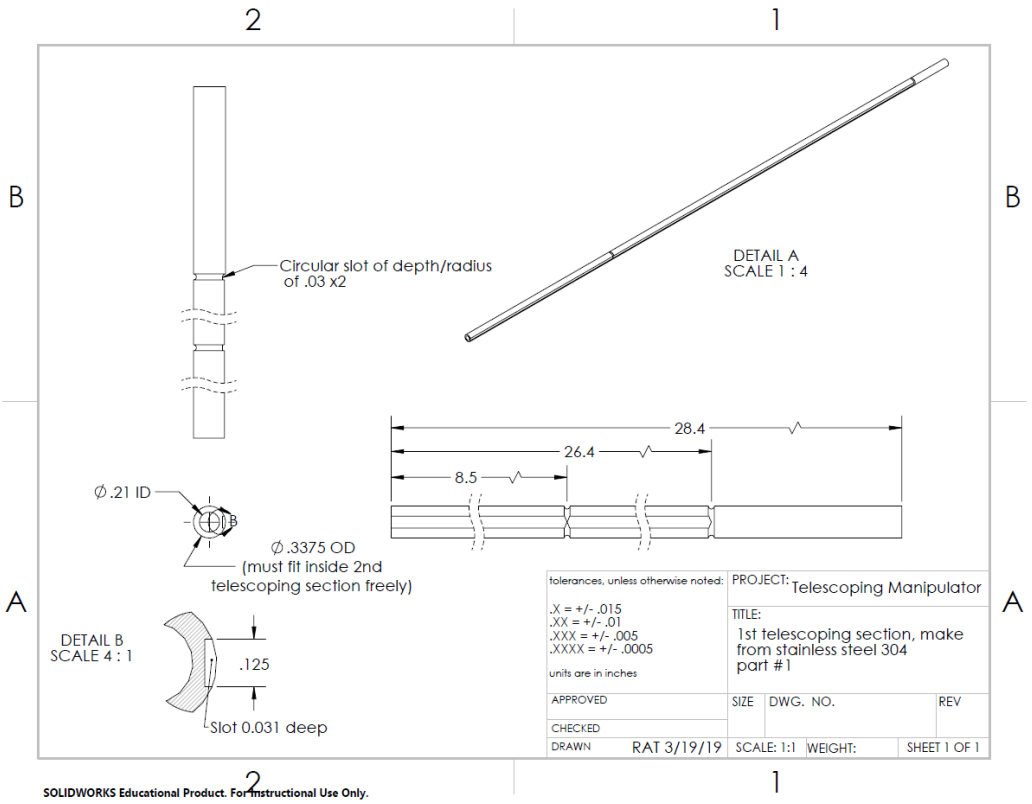

Figure B-5: Inner section for prototype 4: full-scale prototype

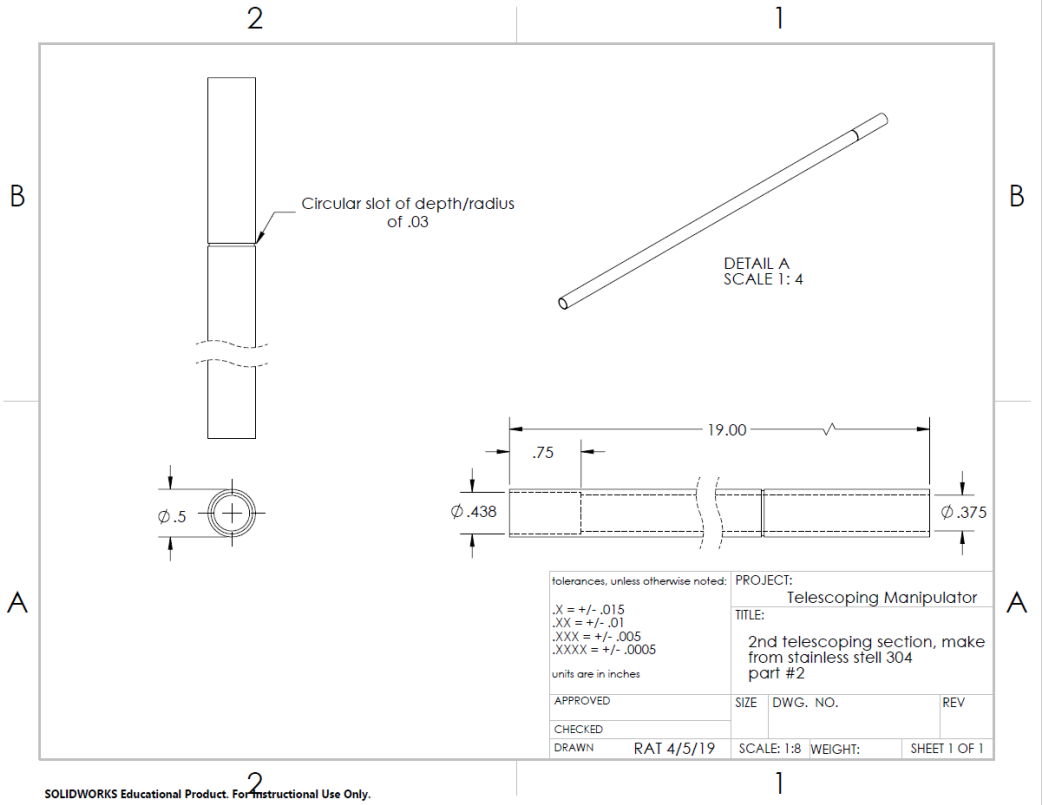

Figure B-6: Outer female section for prototype 4: full-scale prototype

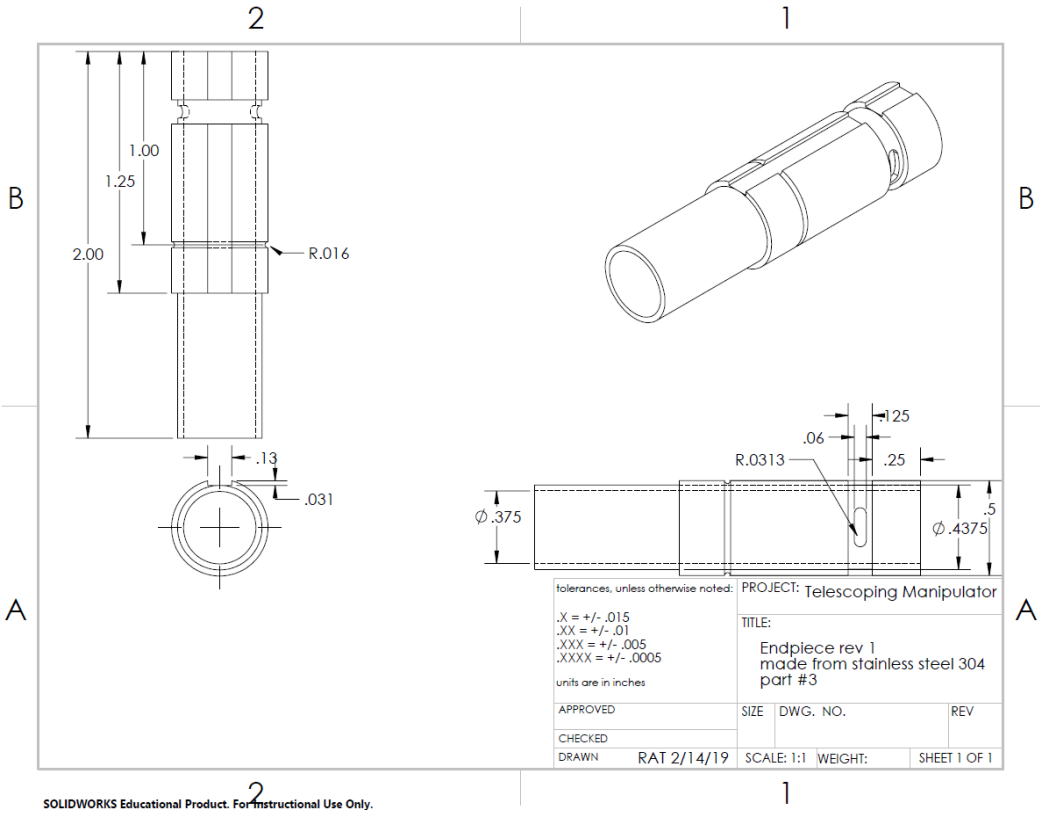

Figure B-7: Endpiece design for prototype 4: full-scale prototype

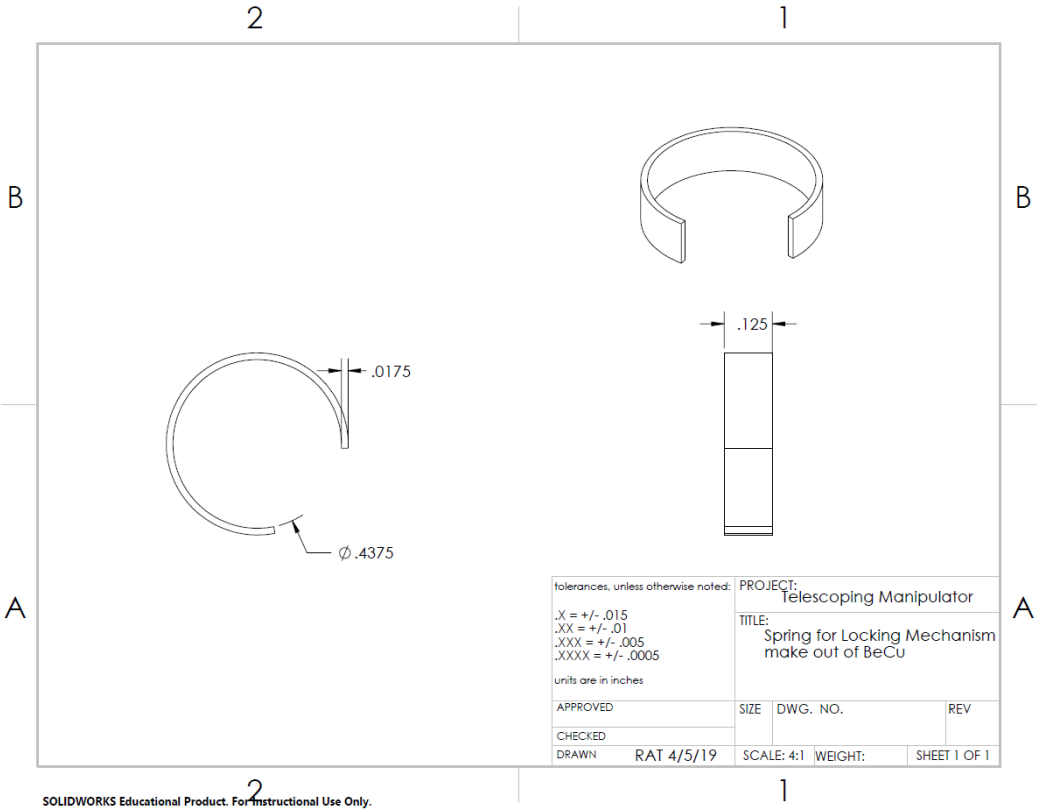

Figure B-8: BeCu C-shaped spring for prototype 4: full-scale prototype

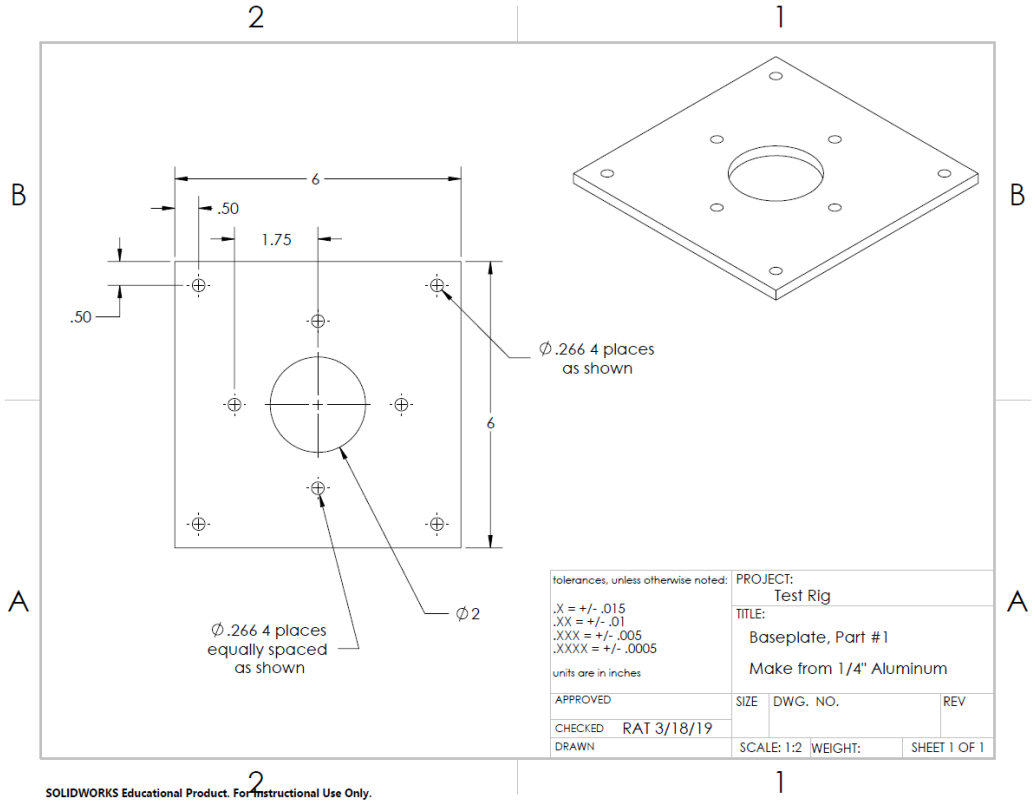

Figure B-9: Water-jet aluminum bracket for test rig

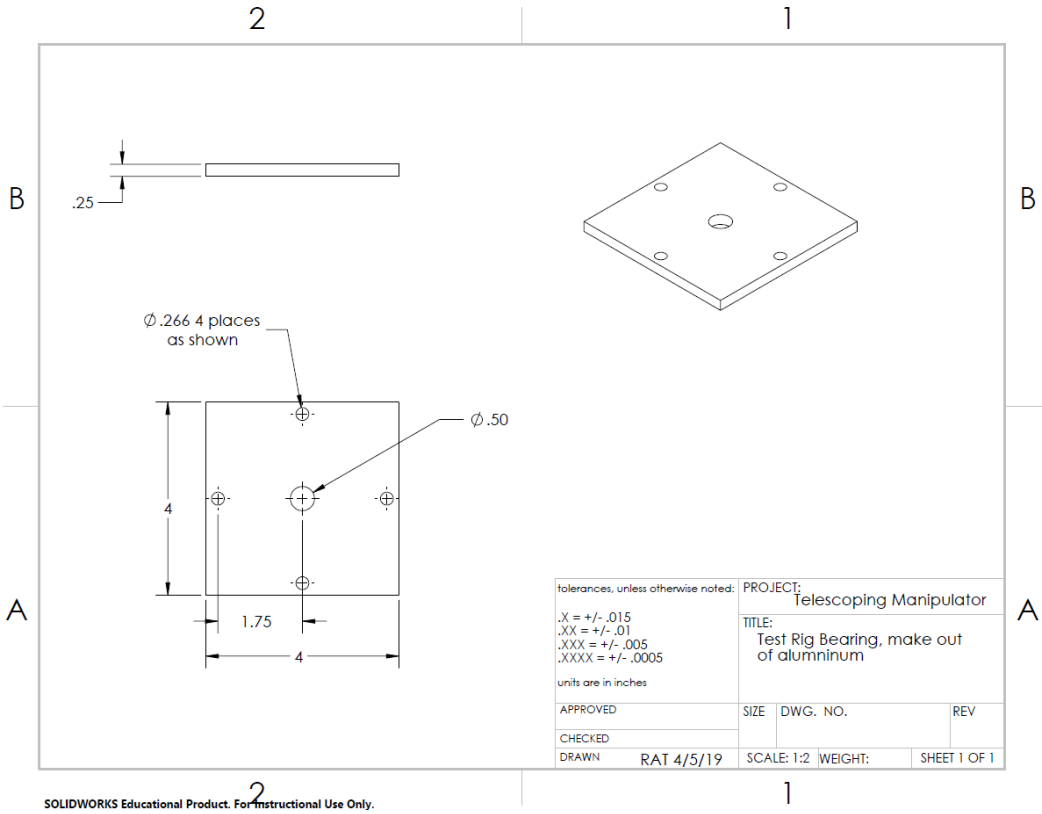

Figure B-10: Aluminum bearing for test rig

C. Previous Work

C.1 COMSOL BeCu Simulations

Spring	Inner Diameter (in)	Thickness (in)	Height (in)	K (N/m) *10^3
1	0.4375	0.0625	0.09375	446.428
2	0.55	0.0625	0.09375	240.963
3	0.4375	0.125	0.09375	2487.56
4	0.4375	0.0625	0.09375	446.428
5	0.4375	0.0625	0.125	610.314
6	0.4375	0.0625	0.25	1255.45

Table C.1

Table C.1 shows the results from a preliminary COMSOL simulation. The conclusion reached from this simulation is that a change in the height and thickness of the BeCu spring have great impacts on the spring constants of the Springs. This is useful to ensure that the locking mechanisms on the telescoping sections lock and unlock in the correct order. By increasing the height and thickness of the springs on the top locking mechanism, the lower locking mechanism will unlock before the top.

These simulations were performed by importing the specified geometries from SolidWorks into COMSOL, fixing in the middle (Figure C-1 (1)) and applying equal forces on either side pad (Figure C-1 (2) and (3)). Then each displacement was measured, and the spring constant is calculated assuming a linear deformation.

$$K = \frac{F}{d}$$

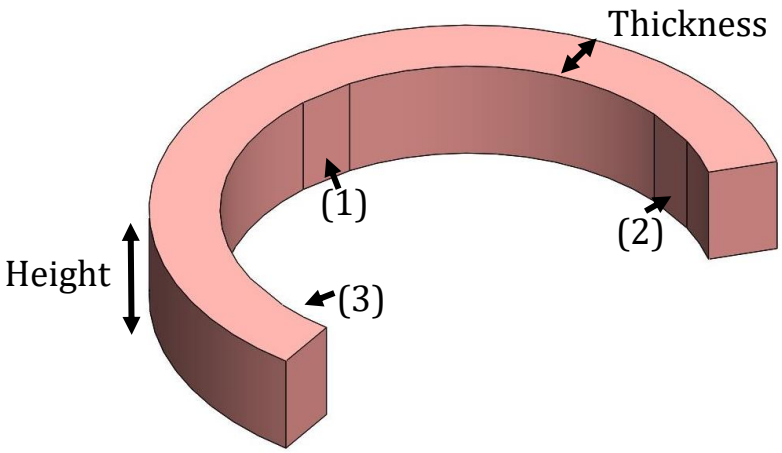

Figure C-1: CAD Model of BeCu Spring. Held Static at (1) with Forces Applied at (2) and (3) Simulated with COMSOL

C.2 BeCu Spring Annealing

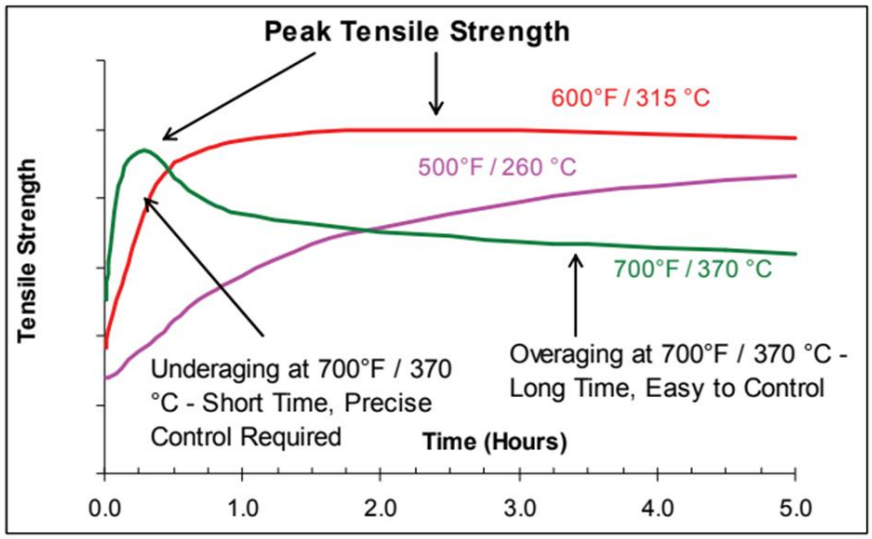

Figure C-2: Time vs Tensile Strength for BeCu Annealing [5]